Food Chemistry 196 (2016) 411–417

Contents lists available at ScienceDirect

Food Chemistry

journal homepage: www.elsevier.com/locate/foodchem

Analytical Methods

Simultaneous imaging of fat crystallinity and crystal polymorphic types by Raman microspectroscopy

Michiyo Motoyama [a,*], Masahiro Ando [b], Keisuke Sasaki [a], Ikuyo Nakajima [a], Koichi Chikuni [a], Katsuhiro Aikawa [a], Hiro-o Hamaguchi [b,c]

[a] NARO Institute of Livestock and Grassland Science, National Agriculture and Food Research Organization (NARO), Ikenodai 2, Tsukuba, Ibaraki 305-0901, Japan
[b] Consolidated Research Institute for Advanced Science and Medical Care, Waseda University, Wakamatsuchou 2-2, Shinjuku, Tokyo 162-8480, Japan
[c] Department of Applied Chemistry, College of Science, National Chiao Tung University, Taiwan, 1001 University Road, Hsinchu 300, Taiwan, Republic of China

ARTICLE INFO

Article history:
Received 11 February 2015
Received in revised form 9 September 2015
Accepted 12 September 2015
Available online 16 September 2015

Keywords:
Raman imaging
Fat crystalline states
Microstructures
Physical properties
Lard
Meat

ABSTRACT

The crystalline states of fats, *i.e.*, the crystallinity and crystal polymorphic types, strongly influence their physical properties in fat-based foods. Imaging of fat crystalline states has thus been a subject of abiding interest, but conventional techniques cannot image crystallinity and polymorphic types all at once. This article demonstrates a new technique using Raman microspectroscopy for simultaneously imaging the crystallinity and polymorphic types of fats. The crystallinity and β′ crystal polymorph, which contribute to the hardness of fat-based food products, were quantitatively visualized in a model fat (porcine adipose tissue) by analyzing several key Raman bands. The emergence of the β crystal polymorph, which generally results in food product deterioration, was successfully imaged by analyzing the whole fingerprint regions of Raman spectra using multivariate curve resolution alternating least squares analysis. The results demonstrate that the crystalline states of fats can be nondestructively visualized and analyzed at the molecular level, *in situ*, without laborious sample pretreatments.

1. Introduction

The physical properties of systems containing fat strongly depend on the crystalline states of the fats—that is, the degrees of crystallinity, the spatial distribution patterns of the crystals, the types of crystal polymorphs, and the higher-order structures formed by the crystals (such as networks and spherulites). In fat-based foods, the crystalline states of the fats determine the products' macroscopic qualities, such as rheological properties, texture, storage performance, and palatability (Ali, Selamat, Man, & Suria, 2001; Bell, Gordon, Jirasublcurtakorn, & Smith, 2007; Marangoni, Narine, Acevedo, & Tang, 2013; Ronholt, Kirkensgaard, Pedersen, Mortensen, & Knudsen, 2012).

The factors affecting the physical properties of a fat-based system have been elucidated, but there are presently no widely accepted models that explain these physical properties despite significant, sustained efforts to construct an appropriate model (Marangoni et al., 2013). This is primarily due to the lack of techniques required to obtain simultaneous images of fat crystallinity and crystal polymorphic type. Simultaneous acquisition is necessary because both crystallization and the polymorphic transformation of fats are kinetic processes. Polarized microscopy, electron microscopy, confocal microscopy, and atomic force microscopy have been used to determine the presence and spatial distribution of fat crystals (Ghosh & Rousseau, 2011; Marangoni et al., 2013; Strobl, 2006), but results obtained using these techniques were inadequate to identify the crystal polymorphic type. Microbeam synchrotron X-ray diffraction has been used to determine polymorphic types (Bayes-Garcia, Calvet, Cuevas-Diarte, Ueno, & Sato, 2011) but does not provide quantitative information. Nuclear magnetic resonance is another possible imaging technique, but its spatial resolution is between ten to one hundred micrometers, which is too large for observing fat crystals.

In contrast, Raman microspectroscopy has the potential for simultaneous imaging of fat crystallinity and crystal polymorphic type, and confocal Raman microspectroscopy easily provides the required spatial resolution of several micrometers. Raman spectra can sharply reflect the molecular structure of fat crystals, such as the all-*trans* configuration of polymethylene chains and crystal subcell structure, allowing the quantitative determination of fat crystallinity and the β′-crystal polymorph (Motoyama, Chikuni, Narita, Aikawa, & Sasaki, 2013). In this study, we build on our previous research and describe the microscopic imaging and separate detection of another major polymorph, β, with the help of a multivariate data analysis approach, multivariate curve resolution

* Corresponding author.
E-mail address: mmichiyo@affrc.go.jp (M. Motoyama).

http://dx.doi.org/10.1016/j.foodchem.2015.09.043
0308-8146/

alternating least squares (MCR-ALS) (Azzouz & Tauler, 2008). New development of a Raman microspectroscopic technique to image the crystallinity, crystal polymorphic types, and higher-order crystal structures of a model fat system is reported.

2. Materials and methods

2.1. Samples

Porcine adipose tissue was used as a model fat system since the phase behavior of porcine fats has been intensely investigated and the expression of multiple crystal polymorphic types has been reported (Campos, Narine, & Marangoni, 2002). Subcutaneous adipose tissue (inner layer, approximately 1-cm thick) covering the dorsal area of the lumber longissimus muscle was obtained after slaughtering a growing-finishing pig (93.4 kg body weight, 5-month old, female) in accordance with international guiding principles (CIOMS, 2012). The experiment was approved by NARO (Approval 11040125). The tissue was kept in a refrigerator at 3.8 ± 2.5 °C for one day to induce a slow-crystallization process (Campos et al., 2002), then a 4 cm × 4 cm area of the tissue was cut into pieces, each piece was sealed with polyethylene film, and frozen at −20 °C until use. Next, the frozen tissue was transferred to the refrigerator for 0 h, 4 h, 10 days, and 2 months prior to Raman microspectroscopic measurement in order to develop changes in the crystalline state of the fat. A standard fat sample, OPO (1,3-dioleoyl-2-palmitoyl-*sn*-glycerol) was purchased (⩾99% purity, Sigma–Aldrich).

2.2. Fatty acid composition analysis

The fatty acid composition of the sample was analyzed to obtain structural information on the polymethylene chains (acyl chains) comprising the fat. Fat was extracted from the adipose tissue with diethylether at approximately 60 °C and its fatty acid composition was analyzed using standard methods (AOCS, 1997, 2001). The composition of the prepared fatty acid methyl esters was analyzed using a gas chromatograph (GC-17A, Shimadzu) equipped with a nitrylsilicon stationary phase capillary column (HR-SS-10, Shinwa Chemical Industries). The amount of each type of acyl chain was expressed as a proportion of the total. Measurement was performed in duplicate.

2.3. Raman microspectroscopic measurement

Prior to the Raman microspectroscopic measurement, the tissues pieces were sliced into sections of approximately 0.5 mm thick in the refrigerator using a surgical knife. The slices were then put on a Peltier control unit whose temperature was set at 0 °C, covered with a glass cover slip to avoid desiccation of the tissue, and dry nitrogen gas was purged over the cover slip to prevent dew condensation. Raman spectra were acquired using a lab-made confocal Raman microspectroscopic system. The 532-nm line of a Nd:YVO_4 laser (Verdi, Coherent) was introduced into an objective lens (LUCPlanFLN20x, Olympus) and focused on the sample. Back-scattered Raman light was collected by the same objective lens and measured with a spectrometer (Shamrock, Andor) equipped with an EMCCD detector (Newton, Andor). The spectral resolution of the system was 2.6 cm^{-1}. The focal point was set to be larger than a fat crystal, 8 μm in diameter and 45 μm in the parallel direction with the optical axis, so as to compensate for the effect of crystal orientation by containing multiple crystals in the focal volume. To minimize the effect, incident laser light was depolarized by passing through a polarization scrambler ($\lambda/4$ plate). The excitation laser power was 5 mW and the signal accumulation time was 10 s for each spectrum. No heating effect was observed in the spectra. A spectrum was obtained at every 4-μm step along with the *x*- and *y*-axes in a microscopic view (52 μm × 72 μm), and a set of Raman spectra for each view was acquired within 40 min. Raman spectra of the standard acylglycerol sample (OPO) were also obtained under the same condition. Random cosmic-ray lines observed in the Raman spectra were removed by comparing spectra.

2.4. Crystallinity imaging

Information on the fat crystallinity was extracted from the obtained Raman spectra and reconstructed into images. The crystallinity of the fat was calculated as the Raman index C_{trans} (Brambilla & Zerbi, 2005; Motoyama et al., 2013).

$$C_{trans} = \frac{(1.3)I_B}{I_{1297} + I_{1305}} \times 100 \quad (1)$$

where I denotes the integrated intensity of the Raman band at the wavenumber identified by a subscript. I_B in the numerator is the intensity of band B (Brambilla & Zerbi, 2005), which is assigned to the in-phase stretch mode of the C–C bonds for all-*trans* polymethylene chains (Schachtschneider & Snyder, 1963; Snyder & Schachtschneider, 1963). Polymethylene chains constituting fat crystals are essentially in an extended, all-*trans* configuration; therefore, I_B corresponds to the mass of the fat crystals. $I_{1297} + I_{1305}$ in the denominator is the spectral internal standard representing the CH_2 twisting intensity arising from all of the CH_2 groups (Brambilla & Zerbi, 2005). The factor 1.3 in this equation is an experimental correction coefficient for the contribution of each CH_2 group of the all-*trans* chains to I_B relative to $I_{1297} + I_{1305}$ (Brambilla & Zerbi, 2005). To obtain the intensity of the target Raman bands, a curve-fitting procedure was applied to the spectral region containing bands that significantly influence the intensity of the target bands. The number of bands in the spectral region was not known exactly so a minimum number of bands was assumed. Pseudo-Voigt function was used for fitting and image smoothing was performed by interpolation using a cubic function.

2.5. β′ crystal polymorphic imaging

The ratio of crystals in the β′ polymorph form to the total fat mass was calculated from the spectra and expressed by the Raman index $\alpha_{\beta'}$ (Motoyama et al., 2013; Mutter, Stille, & Strobl, 1993).

$$\alpha_{\beta'} = \left(\frac{1}{0.493}\right)\frac{I_{1418}}{(I_{1297} + I_{1305})} \times 100 \quad (2)$$

The Raman band at 1418 cm^{-1} originates from the characteristic crystal structure of the β′ polymorph. In β′ crystals, adjacent polymethylene chains align with each other, orienting their plane perpendicularly each other within the polymorph orthorhombic subcell ($O_\perp$) (Sato et al., 1989; Simpson & Hagemann, 1982). I_{1418} in the numerator therefore corresponds to the mass of the β′ crystal polymorph. The factor 1/0.493 is the intensity correction coefficient for I_{1418} relative to $I_{1297} + I_{1305}$ and is experimentally determined (Mutter et al., 1993; Strobl & Hagedorn, 1978).

2.6. β crystal polymorphic imaging

The whole spectral fingerprint region was analyzed to obtain the quantitative information by means of MCR-ALS (Azzouz & Tauler, 2008) conducted on the MATLAB (MathWorks) platform via an interface program written by Tauler's group (Jaumot, Gargallo, de Juan, & Tauler, 2005). MCR-ALS decomposes a data matrix **D** (size c × ν) consisting of experimentally measured

spectra in the rows into the product of two matrices, **C** (size c × n) and $\mathbf{S}^T$ (size n × ν), using a bilinear model:

$$\mathbf{D} = \mathbf{C}\mathbf{S}^T + \mathbf{E} \quad (3)$$

where **E** is the error matrix. The column profiles of **C** and the row profiles of $\mathbf{S}^T$ are associated respectively with the concentrations and pure spectral profiles of the resolved components. MCR-ALS solves Eq. (3) iteratively by an alternating least-squares algorithm that calculates **C** and $\mathbf{S}^T$ that optimally fit **D**. This optimization is carried out by adopting a proposed number of resolved components (n) and an initial estimate of either **C** or $\mathbf{S}^T$ (Azzouz & Tauler, 2008). An initial estimate of **C** was used in the present study. Matrix decomposition was constrained to produce non-negative spectra and concentrations for the resolved components, and the optimization procedure was carried out until convergence (0.1%) was achieved. The number of resolved components (n) was assessed by the eigenvalues obtained from principal component analysis (PCA), given that the non-major components have relatively small eigenvalues. PCA was conducted using SAS software (version 9.3, SAS Institute). Since a larger variance in the experimental data does not always correspond to a greater importance of the variable, PCA was applied to the data in the form of a correlation matrix.

3. Results and discussion

The Raman spectra of the adipose tissue samples were the typical fingerprint spectra of fats (Supporting information, Fig. S1). Raman bands originating from various vibrational modes of the polymethylene chains comprising fat molecules were observed below the 1600-cm^{-1} spectral region and sharply reflected the structural differences between the chains due to crystallization and polymorphic transformation of the fats. The Raman spectral information allowed the simultaneous and quantitative imaging of the crystallinity of the fats and of their crystal polymorphs using the method described below.

3.1. Crystallinity imaging

Fat crystallinity was expressed by a Raman spectroscopic index, C_{trans} (Eq. (1)). To obtain I_B in Eq. (1), it was necessary to identify band B from the multiple bands arising from the various polymethylene chain structure found in fat from living organisms.

Table 1 shows the acyl chain composition of the sample fat. Oleoyl (18:1) and palmitoyl (16:0) are the major acyl chains comprising the fat, and they account for 68.2 weight% of the total acyls. OPO which is comprised of these two acyls and is the most abundant acylglycerol molecule in porcine fat (about 20%) (Motoyama, Ando, Sasaki, & Hamaguchi, 2010; Padley, Gunstone, & Harwood, 1986). Each acyl chain is attached to a glycerol backbone and has a free end (Fig. 1a). Oleoyl (18:1) comprises two nine-carbon polymethylene chains, connected by the C=C bond. Therefore, an OPO molecule has three types of polymethylene chain that provide different vibrational-spectroscopic signatures: a chain of 16 carbons with a free end, a chain of 9 carbons with a free end, and a chain of 9 carbons without a free end. The vibrational frequencies of these polymethylene chains are respectively around 1130, 1122, and 1098 cm^{-1} (Kobayashi, Kaneko, Sato, & Suzuki, 1986; Tasumi & Krimm, 1967) and correspond to the bands indicated by arrows in Fig. 1b.

Table 1
Acyl composition of the fat extracted from the sample adipose tissue measured by gas chromatography.

Acyl	Weight%		s.d.
8:0	0.1	±	0.0
10:0	0.1	±	0.0
12:0	0.2	±	0.0
14:0	1.6	±	0.1
16:0	25.6	±	0.0
16:1	2.3	±	0.1
17:0	0.3	±	0.0
17:1	0.2	±	0.0
18:0	15.8	±	0.4
18:1	42.6	±	0.6
18:2	7.6	±	0.1
18:3	0.7	±	0.0
20:0	0.3	±	0.1
20:1	1.1	±	0.1
20:2	0.5	±	0.0

Acyls are expressed by the two numbers separated by a colon for the chain length (the numbers of carbon atoms) and the number of C=C bonds, respectively.

Several other bands in OPO were detected, around 1090, 1080, 1060, and 1050 cm^{-1} (Fig. 1b). It may be possible to exclude these bands from I_B: the strong band at 1060 cm^{-1} is the out-of-phase stretch mode (Brambilla & Zerbi, 2005), the 1050-cm^{-1} band is likely a progression band of the glycerol side chain of 18:1 (Kobayashi et al., 1986), and 1090 and 1080 cm^{-1} may also be progressions of the 16:0 chain or of the bands derived from a short C–C sequence.

The three major bands observed for OPO at 1130, 1122, and 1098 cm^{-1} were also observed in the spectra of the fat sample, despite the fact that the crystal subcell structure of the fat differs depending on the polymorph types (Kobayashi et al., 1986). The next-most-abundant acyl moiety was 18:0 (15.8 weight%, Table 1) and may have a wavenumber similar to that of 16:0 (1130 cm^{-1}) (Kobayashi et al., 1986; Tasumi & Krimm, 1967). Acyls 18:2 and 16:1 together accounted for about 10 weight% of the total acyls, and their glycerol side chains (nine carbons) corresponded to 1122 cm^{-1}, similar to the glycerol side chain of 18:1 (nine carbons), as described earlier. All other acyl chains accounted for <4 weight% and thus their contribution to the spectrum was likely small. The intensities of the three major bands were therefore integrated to obtain I_B for the fat sample. Eq. (1) was explicitly written as:

$$C_{trans} = \frac{(1.3)(I_{1130} + I_{1122} + I_{1098})}{I_{1297} + I_{1305}} \times 100$$

Broad bands originating from melted fat were also observed and affected the shape and intensity of the three major bands. Curve-fitting procedures were thus performed to obtain C_{trans} using the spectral shape of the melted fat as a fitting component.

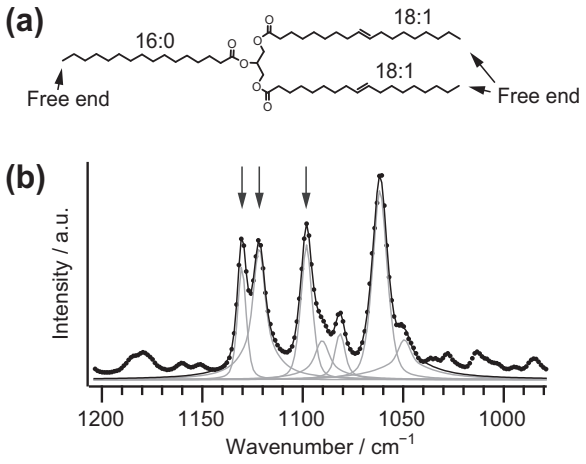

Fig. 1. Structure and spectrum of OPO. (a) One palmitoyl (16:0) and two oleoyls (18:1) are attached to the glycerol backbone. (b) Spectrum of polycrystal of OPO in β polymorphic form. Experimental data (dotted line) and fitting result (black line) with its components (gray line) are shown.

The obtained C_{trans} was reconstructed into images and merged with optical microscopic views (Fig. 2a and b). Raman microspectroscopy visualized fat crystallinity, which previously had been characterized only macroscopically. The distribution of crystallinity was not uniform within the views examined. The differences between the focal points showing the lowest and the highest degrees of crystallinity became more apparent after 10 days of refrigeration. After 2 months, crystallinity increased to approximately 100% in the areas with the highest degrees of crystallinity. Kinetic processes such as crystal growth and Ostwald ripening (the dissolution of small crystals and the growth of large ones, Foubert, Dewettinck, Van de Walle, Dijkstra, & Quinn, 2007) might have proceeded during that period, resulting in the generation and detection of one or more large crystals. The relationship between the distribution of crystallinity and tissue structure (Supporting information, Fig. S2) was unclear. However, increases in crystal size and crystallinity after two months might have been associated with the observed changes, including the obscuration of the tissue structure (Fig. 2a) and the formation of gaps (dark areas in the optical image) due to volume reduction of the system occurring concomitantly with crystallization.

3.2. β′ crystal polymorphic imaging

Crystal polymorphic types were separately imaged. Porcine fats crystallize in the β′ polymorph (Campos et al., 2002). The amount of fat in the form of β′ crystal polymorph ($\alpha_{\beta'}$) were obtained from the Raman spectra and the reconstructed images are shown in Fig. 2c.

The β′ crystals formed a higher-order, colloidal gel network-like structure after 0- and 4-h of refrigeration. The rheological properties of fat systems have been interpreted using network models developed for colloidal gels (Marangoni et al., 2013). The β′ polymorph may contribute significantly to the formation of this network in porcine adipose tissue because the development of a network structure in samples refrigerated for ten days was observed. β′ crystals sinter to each other (Johansson & Bergenstahl, 1995) and the β′ crystals formed during 10 days of refrigeration appeared to reinforce the network structure. This network structure seemed to be affected by the tissue structure.

Network structures retain melt fractions inside them. The maximum concentration of β′ increased further after two months of refrigeration; however, the crystallinity of those pixels was low (Fig. 2b) suggesting the presence of melt fractions in the focal point together with β′ crystals.

3.3. β crystal polymorphic imaging

The sample refrigerated for two months, showed a region with fewer β′ crystals but high crystallinity (Fig. 2b and c), suggesting the presence of crystal types other than β′. The polymorphic transformation of porcine fat into the most stable crystal type, β, occurs easily (Foubert et al., 2007) so the β polymorph was likely generated after two months. No Raman band very specific to the

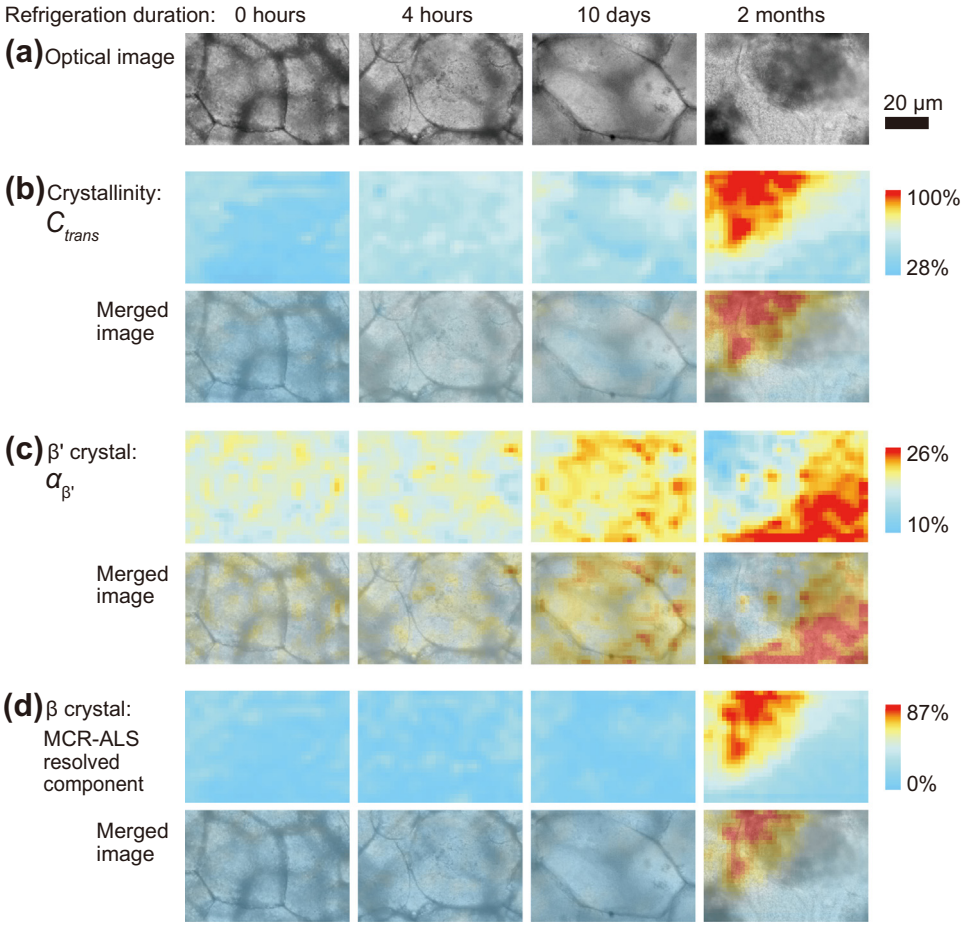

Fig. 2. Simultaneous Raman microspectroscopic imaging of fat crystalline state of porcine adipose tissues refrigerated at 4 °C for different durations. Color scales are ranging from the minimum to the maximum values of the obtained result. (a) Optical microscopic images, (b) C_{trans} corresponding to the fat crystallinity, (c) $\alpha_{\beta'}$ corresponding to the amount of β′ crystal polymorph, (d) concentration profile of an MCR-ALS-resolved component corresponding to β crystal polymorph.

β polymorph has been reported and thus the β crystals could not be quantified from particular bands. The alkyl planes of polymethylene chains in the β crystal are oriented in parallel in a triclinic crystal subcell ($T_{//}$) (Sato, 1999) and should exhibit different inter-chain interactions from other polymorphs. Even a subtle structural difference changes the coupling of vibrations and results in an important difference in the fingerprint region of the spectrum. Therefore, an attempt to comprehensively image the difference appearing in the whole fingerprint spectral dataset was made using MCR-ALS multivariate analysis.

MCR-ALS has been used to decompose multicomponent data into information about each component and has been applied in spectroscopy to extract quantitative information on spectral components (Zhang et al., 2013). Importantly, the validity of the decomposition result can be verified by checking whether or not the spectra of the resolved components are physically meaningful.

The number of components to be resolved (n) was determined prior to the MCR-ALS analysis by PCA using the data obtained for all 936 spectra. The results showed that three principal components (PCs) could explain at least 1% of the variance of the spectral data (cumulative variance explained 93.8% of the variance). This means that there were approximately three spectroscopically different components in the data set, although the fat sample contained many acylglycerol molecular species. Decomposition of experimental data by MCR-ALS requires an initial estimate of the concentrations or spectra of those components should be given properly in order to avoid local minima or rotational ambiguity of the matrix decomposition. Three components were identified from PCA.

Eigenvectors of the first PC were essentially a flat line (Fig. 3), indicating that the most variation in the spectra arose from baseline fluctuation and that no characteristics were apparently related to fat.

The peaks in the eigenvector of the second PC (Fig. 3) corresponded to fat crystals. As described in Section 3.1, the peaks at 1098 and 1122 cm^{-1} are the in-phase stretch modes of the all-*trans* C–C sequences in crystals, and the peak at 1060 cm^{-1} is the out-of-phase stretch mode of the sequences. The peak at 686 cm^{-1} corresponds to the C=C–H out-of-plane bend mode of the fat crystals having acyl chains with a C=C bond, such as 18:1 (Tandon, Forster, Neubert, & Wartewig, 2000). Troughs in the eigenvector of the second PC correspond to melt fat since 1302 cm^{-1} is the CH_2 twist mode which is prominent in the melt phase (Zerbi, Conti, Minoni, Pison, & Bigotto, 1987). The broad shapes of the troughs at around 1075 and 835 are melt-specific superimposed progressions of the density of the state (Cates, Strauss, & Snyder, 1994; Snyder, 1967). The trough at 1648 cm^{-1} is due to C=C stretching and is consistent with the fact that an acylglycerol species with a high degree of unsaturation and a low melting point being present in the melt phase even at refrigeration temperatures. The trough at 1755 cm^{-1} is the C=O stretching mode and corresponds to the band observed in the melt (Da Silva & Rousseau, 2008). Together, these results indicated that the second PC corresponds to the dynamic change between the melt phase and the crystal phase.

Peaks corresponding to Raman bands specific to the β′ crystal polymorph are observed in the third PC. The peak at 1418 cm^{-1} originates from the crystal subcell structure of β′, as described in Section 2.5. The troughs correspond to bands due to the β polymorph, since troughs at 1744, 1728, and 1470 cm^{-1} were observed in the β polymorphs of several acylglycerol species and the trough at 1744 may also be observed in melt (Sato et al., 1989; Simpson & Hagemann, 1982). The third PC is therefore likely compatible with the spectral difference between β′ and β, the major polymorphs of porcine fat.

The three spectroscopically different components were therefore identified as the melt and two crystal polymorphs, β′ and β. The acylglycerol species with low melting temperatures were likely in the melt phase and those with high melting temperatures crystallized, each forming a suitable subcell structure ($O_{\perp}$ or $T_{//}$) as a function of its chemical potential.

The initial conditions for MCR-ALS matrix decomposition were the estimated concentrations of the three components; these estimates were derived from the Raman indexes: $100 - C_{trans}$ for melt, $\alpha_{\beta'}$ for β′ crystal, and the remaining ($C_{trans} - \alpha_{\beta'}$) for β crystal by subtracting $100 - C_{trans}$ and $\alpha_{\beta'}$ from 100. The initial estimates are not necessarily exact because MCR-ALS optimization processes minimize the lack of fit. Three components with the spectra shown in Fig. 4 were acquired. The percent of variance explained (R^2) was 99.4% and the lack of fit with experimental data (Jaumot et al., 2005) was 7.5%. Data were adequately explained by the model

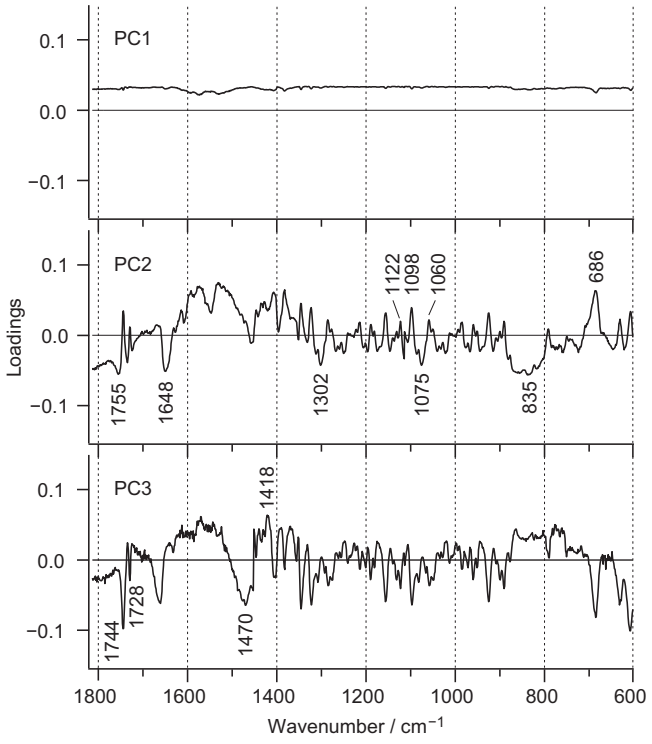

Fig. 3. Eigenvectors for the three principal components of the experimental data set.

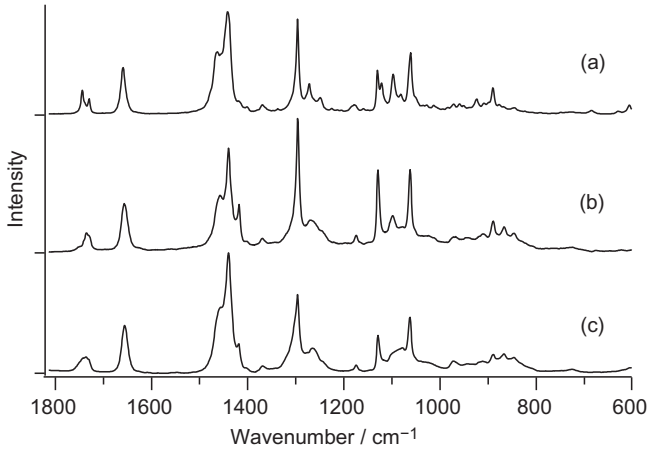

Fig. 4. Result of the MCR-ALS matrix decomposition, showing the acquired spectral profiles for the three resolved components. The spectral components whose concentrations are estimated: (a) $C_{trans} - \alpha_{\beta'}$, (b) $\alpha_{\beta'}$ and (c) $100 - C_{trans}$, respectively.

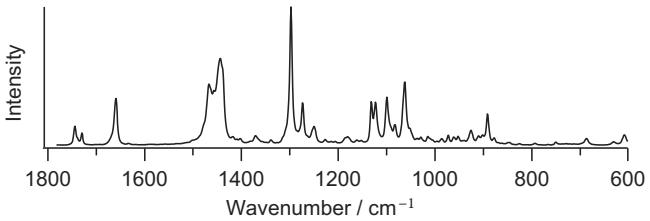

Fig. 5. Spectrum of β crystal polymorph of OPO.

adopting $n = 3$ and the initial condition. The acquired spectra (Fig. 4) showed natural shapes indicating that the decomposition was successful.

The acquired spectral profile for β crystal (Fig. 4a) closely resembled the spectrum of OPO (Fig. 5). Porcine fat contains acylglycerol species with high structural similarity to OPO such as OSO (1,3-dioleoyl-2-stearoyl-*sn*-glycerol, 1.2 mol%) and OMO (1,3-dioleoyl-2-myristoyl-*sn*-glycerol, 1.6 mol%) with stearoyl (18:0, S) or myristoyl (14:0, M) in place of 16:0, respectively (Padley et al., 1986). Acylglycerol species with similar properties mix to form a continuous solid solution (Timms, 2003). MCR-ALS likely extracted the spectrum of the β crystal of OPO accompanied by these minor acylglycerol species, maybe explaining the minor inconsistency existing in the spectral profiles (Figs. 4a and 5). The amount of β crystal in the sample would be a few percent higher than the amount of OPO (c.a. 20%) for due to the presence of acylglycerol species with high similarity to OPO.

An image of a β crystal was reconstructed (Fig. 2d) and shows irregular patchy patterns rather than the uniformly spread network of a colloidal gel. The β crystals were highly localized as spherical structures in the region showing very high crystallinity in the two month refrigerated sample. β crystals form large spherulitic aggregates (~100 μm) (Heertje & Lewis, 1993) and it is these aggregates that may have been imaged. Large structures often cause graininess, a defect in fat-based products. Moreover, β-polymorph formation generally decreases the firmness of the products, often considerably and is probably associated with the observed patchy and discontinuous structure, disturbing the continuity of the β′ crystal.

The other two spectral profiles (Figs. 4b and c) displayed the characteristics of the β′ crystal and melt, respectively. The obtained spectral profile for β′ (Fig. 4b) had a strong 1418-cm^{-1} band, specific to the type of polymorph (Section 2.5). The spectral profile as a whole agreed well with spectra reported previously (Da Silva, Bresson, & Rousseau, 2009; Sprunt, Jayasooriya, & Wilson, 2000). The profile for melted fat (Fig. 4c) showed the spectral features of melt reported earlier (Brambilla & Zerbi, 2005; Da Silva et al., 2009) but also had characteristics of crystals, *e.g.*, sharp bands at 1130 and 1060 cm^{-1} originating from the all-*trans* C–C sequence. Small crystals were likely dispersed in the melt fraction or transient structures of a melt-crystal boundary may have coexisted with the melt (Mutter et al., 1993) and were thus inseparable from the melt. It may be possible to obtain the spectral profile of the melt by increasing the spatial resolution of the Raman microspectroscopic system.

MCR-ALS matrix decomposition can also adopt spectra as the initial condition. If the spectra of all major components of the system are known in advance, the expected result will be obtained straightforwardly as previously demonstrated (for example, Zhang et al., 2013). However, the validity of the obtained concentration profile will be difficult to check as only the current Raman technique can quantify the type of crystal polymorph with spatial resolution. Consequently, checking the validity of the results by evaluating the obtained spectral profile, as demonstrated in the present study, is likely the only way at present to visualize a fat crystalline state quantitatively.

3.4. Potential of the Raman microspectroscopic technique for fat imaging

Although infrared spectroscopic imaging can provide a fingerprints spectrum and perhaps can be used as a simultaneous imaging technique, Raman imaging is superior because: (a) it provides higher spatial resolution (up to 300 nm) since Raman spectroscopy uses a shorter wavelength light; and (b) Raman spectroscopy is largely unaffected by the presence of water in food samples by virtue of its selection rule (Herrero, 2008).

The current technique has some limitations, including the inability to distinguish a particular acylglycerol species. As mentioned previously, the detected β crystal may not be composed of only a single acylglycerol species but rather may also contain other species. A melt or solid solution containing more than one acylglycerol species is considered as a single state comprising acylglycerol species mixed uniformly or become integrated into the same crystallization behavior. The differentiating acylglycerol species is not always required to understand the physical properties of fat. Natural fats cannot be considered in terms of their individual component acylglycerols, but only in terms of their different states (Timms, 2003). It is important to divide the acylglycerol species into states exhibiting distinctive properties, such as melt and types of crystal, to detect the formed structures that dictate the physical properties of the natural fat. It can be said that Raman spectroscopy is suitable for this purpose.

4. Conclusions

The present study demonstrates that simultaneous images of a fat crystalline state can be obtained by analyzing Raman spectra, which contain significant structural information. This Raman spectroscopic technique does not require sample pre-treatment such as dyeing, labeling, or the use of any contrast-enhancing agents, and enables investigation of the crystalline state in a nondestructive, *in situ* manner. The degree of crystallinity and the type and amount of major crystal polymorphs that decisively influence the physical properties of a fat system can be imaged simultaneously. This technique will be useful for unveiling and understanding the mechanisms underlying the formation of physical properties of fat-based foods.

Conflict of interest

The authors declare no competing financial interest.

Acknowledgments

This work was partly supported by JSPS KAKENHI Grant Numbers 24380148 and 25850098; by the Science and Technology Research Promotion Program for Agriculture, Forestry, Fisheries, and Food Industry, number 25064C; and by NIMS Molecule & Materials Synthesis Platform as a "Nanotechnology Platform" program of the Ministry of Education, Culture, Sports, Science, and Technology (MEXT), Japan. M.M. is grateful to Emeritus Prof. Dr. Kiyotaka Sato of Hiroshima University for his invaluable comments on the results and manuscript; to Dr. Takashi Minowa and Dr. Taro Takemura of the National Institute of Material Science (NIMS) for their technical assistance; to the Agriculture, Forestry, and Fisheries Research Information Technology Center (AFFRIT), Japan, for their support in data analysis; and to Dr. Mika Oe and Ms. Yumiko Endo of NARO for their support in the experiments.

Appendix A. Supplementary data

Supplementary data associated with this article can be found, in the online version, at http://dx.doi.org/10.1016/j.foodchem.2015.09.043.

References

Ali, A., Selamat, J., Man, Y. B. C., & Suria, A. M. (2001). Effect of storage temperature on texture, polymorphic structure, bloom formation and sensory attributes of filled dark chocolate. *Food Chemistry, 72*(4), 491–497.

AOCS (1997). *American Oil Chemists' Society Official Method Ce 2-66*. Preparation of methyl esters of fatty acids.

AOCS (2001). *American Oil Chemists' Society Official Method Ce 1e-91*. Determination of fatty acids in edible oils and fats by capillary GLC.

Azzouz, T., & Tauler, R. (2008). Application of multivariate curve resolution alternating least squares (MCR-ALS) to the quantitative analysis of pharmaceutical and agricultural samples. *Talanta, 74*(5), 1201–1210.

Bayes-Garcia, L., Calvet, T., Cuevas-Diarte, M. A., Ueno, S., & Sato, K. (2011). Heterogeneous microstructures of spherulites of lipid mixtures characterized with synchrotron radiation microbeam X-ray diffraction. *CrystEngComm, 13*(22), 6694–6705.

Bell, A., Gordon, M. H., Jirasublcurtakorn, W., & Smith, K. W. (2007). Effects of composition on fat rheology and crystallisation. *Food Chemistry, 101*(2), 799–805.

Brambilla, L., & Zerbi, G. (2005). Local order in liquid *n*-alkanes: Evidence from Raman spectroscopic study. *Macromolecules, 38*(8), 3327–3333.

Campos, R., Narine, S. S., & Marangoni, A. G. (2002). Effect of cooling rate on the structure and mechanical properties of milk fat and lard. *Food Research International, 35*(10), 971–981.

Cates, D. A., Strauss, H. L., & Snyder, R. G. (1994). Vibrational modes of liquid *n*-alkanes: Simulated isotropic Raman spectra and band progressions for C5H12-C20H42 and C16D34. *Journal of Physical Chemistry, 98*(16), 4482–4488.

CIOMS and ICLAS (2012). *International guiding principles for biomedical research involving animals*.

Da Silva, E., Bresson, S., & Rousseau, D. (2009). Characterization of the three major polymorphic forms and liquid state of tristearin by Raman spectroscopy. *Chemistry and Physics of Lipids, 157*(2), 113–119.

Da Silva, E., & Rousseau, D. (2008). Molecular order and thermodynamics of the solid–liquid transition in triglycerides *via* Raman spectroscopy. *Physical Chemistry Chemical Physics, 10*(31), 4606–4613.

Foubert, I., Dewettinck, D., Van de Walle, D., Dijkstra, A. J., & Quinn, P. J. (2007). Physical properties: Structural and physical characteristics. In F. D. Gunstone, J. L. Harwood, & A. J. Dijkstra (Eds.), *The lipid handbook* (3rd ed., pp. 471–534). Boca Raton, FL: CRC Press.

Ghosh, S., & Rousseau, D. (2011). Fat crystals and water-in-oil emulsion stability. *Current Opinion in Colloid & Interface Science, 16*(5), 421–431.

Heertje, I., & Lewis, D. F. (1993). Structure and function of food products: A review. *Food Structure, 12*(3), 343–364.

Herrero, A. M. (2008). Raman spectroscopy a promising technique for quality assessment of meat and fish: A review. *Food Chemistry, 107*(4), 1642–1651.

Jaumot, J., Gargallo, R., de Juan, A., & Tauler, R. (2005). A graphical user-friendly interface for MCR-ALS: A new tool for multivariate curve resolution in MATLAB. *Chemometrics and Intelligent Laboratory Systems, 76*(1), 101–110.

Johansson, D., & Bergenstahl, B. (1995). Sintering of fat crystal networks in oil during post-crystallization processes. *Journal of the American Oil Chemists Society, 72*(8), 911–920.

Kobayashi, M., Kaneko, F., Sato, K., & Suzuki, M. (1986). Vibrational spectroscopic study on polymorphism and order–disorder phase-transition in oleic-acid. *Journal of Physical Chemistry, 90*(23), 6371–6378.

Marangoni, A., Narine, S. S., Acevedo, N., & Tang, D. (2013). Nanostructure and microstructure of fats. In A. Marangoni & L. H. Wesdorp (Eds.), *Structure and properties of fat crystal networks* (pp. 173–232). Boca Raton: CRC Press.

Motoyama, M., Ando, M., Sasaki, K., & Hamaguchi, H.-O. (2010). Differentiation of animal fats from different origins: Use of polymorphic features detected by Raman spectroscopy. *Applied Spectroscopy, 64*(11), 1244–1250.

Motoyama, M., Chikuni, K., Narita, T., Aikawa, K., & Sasaki, K. (2013). *In situ* Raman spectrometric analysis of crystallinity and crystal polymorphism of fat in porcine adipose tissue. *Journal of Agricultural and Food Chemistry, 61*(1), 69–75.

Mutter, R., Stille, W., & Strobl, G. (1993). Transition regions and surface melting in partially crystalline polyethylene: A Raman spectroscopic study. *Journal of Polymer Science Part B-Polymer Physics, 31*(1), 99–105.

Padley, F. B., Gunstone, F. D., & Harwood, J. L. (1986). Occurrence and characteristics of oils and fats. In F. D. Gunstone, J. L. Harwood, & F. B. Padley (Eds.). *The lipid handbook* (1st ed.), pp. 49–170). London: Chapman and Hall.

Ronholt, S., Kirkensgaard, J. J. K., Pedersen, T. B., Mortensen, K., & Knudsen, J. C. (2012). Polymorphism, microstructure and rheology of butter. Effects of cream heat treatment. *Food Chemistry, 135*(3), 1730–1739.

Sato, K. (1999). Solidification and phase transformation behaviour of food fats – A review. *Fett-Lipid, 101*(12), 467–474.

Sato, K., Arishima, T., Wang, Z. H., Ojima, K., Sagi, N., & Mori, H. (1989). Polymorphism of POP and SOS. 1. Occurrence and polymorphic transformation. *Journal of the American Oil Chemists Society, 66*(5), 664–674.

Schachtschneider, J. H., & Snyder, R. G. (1963). Vibrational analysis of the *n*-paraffins—II. Normal co-ordinate calculations. *Spectrochimica Acta, 19*(1), 117–168.

Simpson, T. D., & Hagemann, J. W. (1982). Evidence of two β phases in tristearin. *Journal of the American Oil Chemists Society, 59*(4), 169–171.

Snyder, R. G. (1967). Vibrational study of chain conformation of liquid *n*-paraffins and molten polyethylene. *Journal of Chemical Physics, 47*(4), 1316–1360.

Snyder, R. G., & Schachtschneider, J. H. (1963). Vibrational analysis of the *n*-paraffins—I. Assignments of infrared bands in the spectra of C_3H_8 through *n*-$C_{19}H_{40}$. *Spectrochimica Acta, 19*(1), 85–116.

Sprunt, J. C., Jayasooriya, U. A., & Wilson, R. H. (2000). A simultaneous FT-Raman-DSC (SRD) study of polymorphism in *sn*-1,3-distearoyl-2-oleoylglycerol (SOS). *Physical Chemistry Chemical Physics, 2*(19), 4299–4305.

Strobl, G. (2006). Crystallization and melting of bulk polymers: New observations, conclusions and a thermodynamic scheme. *Progress in Polymer Science, 31*(4), 398–442.

Strobl, G. R., & Hagedorn, W. (1978). Raman-spectroscopic method for determining crystallinity of polyethylene. *Journal of Polymer Science Part B-Polymer Physics, 16*(7), 1181–1193.

Tandon, P., Forster, G., Neubert, R., & Wartewig, S. (2000). Phase transitions in oleic acid as studied by X-ray diffraction and FT-Raman spectroscopy. *Journal of Molecular Structure, 524*, 201–215.

Tasumi, M., & Krimm, S. (1967). Crystal vibrations of polyethylene. *Journal of Chemical Physics, 46*(2), 755–766.

Timms, R. E. (2003). *Confectionary fats handbook. Properties, production and application*. Bridgwater, U.K.: The Oily Press.

Zerbi, G., Conti, G., Minoni, G., Pison, S., & Bigotto, A. (1987). Premelting phenomena in fatty acids: An infrared and Raman study. *Journal of Physical Chemistry, 91*(9), 2386–2393.

Zhang, D. L., Wang, P., Slipchenko, M. N., Ben-Amotz, D., Weiner, A. M., & Cheng, J. X. (2013). Quantitative vibrational imaging by hyperspectral stimulated Raman scattering microscopy and multivariate curve resolution analysis. *Analytical Chemistry, 85*(1), 98–106.